MOLECULAR AND CELLULAR BIOLOGY, July 2002, p. 5100–5113 Vol. 22, No. 14
0270-7306/02/$04.00+0 DOI: 10.1128/MCB.22.14.5100–5113.2002

Astrocyte-Specific Inactivation of the Neurofibromatosis 1 Gene (*NF1*) Is Insufficient for Astrocytoma Formation

Michaela Livia Bajenaru,[1] Yuan Zhu,[2] Nicolé M. Hedrick,[1] Jessica Donahoe,[1] Luis F. Parada,[2] and David H. Gutmann[1]*

Department of Neurology, Washington University School of Medicine, St. Louis, Missouri,[1] and Center for Developmental Biology and Kent Waldrep Foundation Center for Basic Research on Nerve Growth and Regeneration, University of Texas Southwestern Medical Center, Dallas, Texas[2]

Received 19 February 2002/Returned for modification 4 April 2002/Accepted 19 April 2002

Individuals with the neurofibromatosis 1 (NF1) inherited tumor syndrome develop low-grade gliomas (astrocytomas) at an increased frequency, suggesting that the *NF1* gene is a critical growth regulator for astrocytes. In an effort to determine the contribution of the *NF1* gene product, neurofibromin, to astrocyte growth regulation and NF1-associated astrocytoma formation, we generated astrocyte-specific *Nf1* conditional knockout mice (*Nf1*^{GFAP}*CKO*) by using Cre/LoxP technology. Transgenic mice were developed in which Cre recombinase was specifically expressed in astrocytes by embryonic day 14.5. Successive intercrossing with mice bearing a conditional *Nf1* allele *(Nf1flox)* resulted in *GFAP-Cre Nf1flox/flox* (*Nf1*^{GFAP}*CKO*) animals. No astrocytoma formation or neurological impairment was observed in *Nf1*^{GFAP}*CKO* mice after 20 months, but increased numbers of proliferating astrocytes were observed in several brain regions. To determine the consequence of *Nf1* inactivation at different developmental times, the growth properties of embryonic day 12.5 and postnatal day 2 *Nf1* null astrocytes were analyzed. *Nf1* null astrocytes exhibited increased proliferation but lacked tumorigenic properties in vitro and did not form tumors when injected into immunocompromised mouse brains in vivo. Collectively, our results suggest that loss of neurofibromin is not sufficient for astrocytoma formation in mice and that other genetic or environmental factors might influence NF1-associated glioma tumorigenesis.

Neurofibromatosis 1 (NF1) is the most common cancer predisposition syndrome affecting the nervous system, with an incidence of 1 in 3,500 births worldwide (16). Early in life, individuals with NF1 develop café-au-lait spots, skinfold freckling, and iris hamartomas (Lisch nodules). In addition, approximately 15 to 20% of children with NF1 develop glial cell tumors (astrocytomas) involving the optic nerve, chiasm, hypothalamus, and brain stem (31). Although classified as grade I juvenile pilocytic astrocytomas, these tumors can be associated with significant morbidity as a result of visual loss or neurological compromise.

Since individuals affected with NF1 develop tumors at an increased frequency, the *NF1* gene is hypothesized to function as a tumor suppressor. Identification of the *NF1* gene (10, 42, 43) and its protein product, the 220- to 250-kDa cytoplasmic neurofibromin protein, revealed that a small portion of the molecule has sequence similarity with the catalytic domain of a family of proteins termed GTPase-activating proteins (GAPs) (4, 34, 45). GAP molecules function as negative regulators of small mitogenic GTPase proteins, like p21^{ras}, and inactivate these signaling proteins by accelerating their conversion from active, GTP-bound conformations to inactive, GDP-bound forms (6). In NF1-associated tumors, loss of neurofibromin results in increased p21^{ras} mitogenic signaling and augments cell proliferation, leading to tumor formation (5, 7, 12).

* Corresponding author. Mailing address: Department of Neurology, Washington University School of Medicine, Box 8111, 660 South Euclid Avenue, St. Louis, MO 63110. Phone: (314) 362-7379. Fax: (314) 362-2388. E-mail: gutmannd@neuro.wustl.edu.

In support of a role for neurofibromin as a negative astrocyte growth regulator, we have previously demonstrated that neurofibromin expression increases during astrocyte growth arrest in vitro (18). In addition, neurofibromin expression is absent in symptomatic NF1-associated pilocytic astrocytomas, consistent with the notion that homozygous inactivation of the *NF1* gene is associated with astrocytoma formation in NF1 (19). Moreover, in one NF1 patient astrocytoma, loss of neurofibromin expression was associated with increased levels of activated p21^{ras} (28). However, it is not known whether loss of neurofibromin is sufficient for astrocytoma formation.

Mice with targeted disruption of the *Nf1* gene have been developed. Mice heterozygous for a mutated *Nf1* gene (*Nf1*$^{+/-}$ mice) develop several types of tumors, including pheochromocytomas and lymphoid leukemias (8, 24). Despite the absence of astrocytomas in these mice, *Nf1*$^{+/-}$ mice exhibit a 1.5-fold increase in astrocyte proliferation in vivo (18). This heterozygote growth advantage is specific to astrocytes and not seen in oligodendrocytes or microglia. Moreover, heterozygosity for another p21^{ras}-GAP molecule, p120-GAP, does not result in increased astrocyte proliferation in vivo. We further demonstrated that this growth advantage is cell autonomous, in that *Nf1*$^{+/-}$ astrocytes proliferate faster in vitro than wild-type littermate astrocytes and exhibit elevated p21^{ras} pathway activation (3). The lack of astrocytic tumors in *Nf1*$^{+/-}$ mice may reflect the need for further genetic alterations, such as inactivation of the other *Nf1* allele or loss of other tumor suppressor genes.

Genetic cooperativity between the *Nf1* tumor suppressor and other tumor suppressor genes important in sporadic as-

trocytoma pathogenesis (p53 and Rb) has been demonstrated. Heterozygosity for both *Nf1* and *p53* or *Rb* confers a significant growth advantage to brain astrocytes: $Nf1^{+/-}$ $p53^{+/-}$ mice exhibit a threefold increase in astrocyte proliferation in vivo, while $Nf1^{+/-}$ $Rb^{+/-}$ mice exhibit a 2.5-fold increase in astrocyte proliferation in vivo compared to wild-type mice (3). Combined loss of both *Nf1* and *p53* was shown to result in high-grade malignant astrocytoma (glioblastoma) formation (39), different from the benign pilocytic astrocytomas in individuals with NF1 who do not harbor p53 mutations (23, 30).

Germ line homozygosity for an *Nf1* mutation ($Nf1^{-/-}$) results in embryonic lethality between days 12.5 and 14.5 of gestation, secondary to a cardiac vessel defect (8, 24). Because these mice die during mid-embryonic development, the effect of absent neurofibromin expression on normal astrocyte differentiation and the development of astrocytomas cannot be directly addressed. The recent development of *Nf1* conditional mutant mice (*Nf1flox/flox* mice) by using Cre/LoxP technology now permits such an analysis (48).

The first tissue-specific *Nf1* conditional knockout mouse was generated by inactivation of the *Nf1* gene in differentiated neurons by using the synapsin I promoter ($NF1^{Syn1}KO$) (48). $NF1^{Syn1}KO$ mice exhibited reduced forebrain weight, changes in neuronal physiology, activation of the $p21^{ras}$/mitogen-activated protein kinase pathway in neurons, and massive astrogliosis in the cerebral cortex, hippocampus, and brain stem. The astrocytes in these brain areas were not proliferating and demonstrated morphological changes suggestive of reactive astrocytes. Although this mouse model represents an excellent model to study the learning disabilities associated with NF1, $NF1^{SynI}KO$ mice were tumor-free and did not develop astrocytomas.

The development of a mouse model for NF1-associated astrocytomas is an important first step for future translational research efforts relevant to these common tumors in individuals with NF1. In this report, we describe the development of several astrocyte-specific Cre (GFAP-Cre) transgenic mouse lines, the generation of astrocyte-specific *Nf1* conditional knockout mice ($Nf1^{GFAP}CKO$ mice), and characterization of the effects of *Nf1* inactivation at different developmental periods on astrocyte growth and tumor formation. Our results suggest that *Nf1* inactivation alone may not be sufficient for astrocytoma formation in mice.

MATERIALS AND METHODS

Transgenic mice. GFAP-Cre-IRES-LacZ transgenic mice (GFAP-Cre mice) were generated by pronuclear injection of the purified, linearized 8-kbp GFAP-Cre-internal ribosome entry site (IRES)-*lacZ* DNA fragment into C57BL/6 × CBA fertilized mouse eggs by using standard techniques in the Neuroscience Transgenic Facility at the Washington University School of Medicine. The transgene construct consists of the 2.2-kb fragment of the human glial fibrillary acidic protein (GFAP) promoter (Gfa2) (obtained from M. Brenner, National Institute of Neurological Disorders and Stroke) (9), the encephalomyocarditis virus IRES, the cDNA encoding the nucleus-targeted Cre recombinase (provided by J. Milbrandt, Washington University, St. Louis, Mo.) (26), and the cDNA encoding a nucleus-targeted LacZ, followed by the simian virus 40 polyadenylation signal (provided by A. Nagy, Mount Sinai Hospital, Toronto, Canada). The IRES-LacZ allows for cotranslation of the Cre and LacZ proteins from the same mRNA and permits indirect detection of the Cre expression pattern in vivo.

Transgenic mice carrying the GFAP-Cre-IRES-LacZ transgene were identified by tail DNA PCR from 1-week-old mice or from embryonic tail or amniotic tissue by using Cre- and LacZ-specific primers. Briefly, mouse tails were treated with 200 μl of tail extraction buffer (50 mM Tris-HCl [pH 7.4], 1 mM $CaCl_2$, 1% Tween 20) plus 25 μl of 1% proteinase K at 55°C overnight. Then 1 μl of tail DNA was subjected to PCR amplification with the following primers and conditions: CRE, 5′-GTGTCCAATTTACTGACCGTACAC-3′ and 5′-CTAATCG CCATCTTCCAGCAG-3′, at an annealing temperature of 60°C for 30 cycles; and LACZ, 5′-CCAGCTGGCGTAATAGCGAAG-3′ and 5′-CATCGTAACC GTGCATCTGCC-3′, at an annealing temperature of 62°C for 38 cycles.

The PCR results were confirmed by Southern blotting. A total of 10 μg of tail genomic DNA, digested with *Bgl*II and *Not*I to excise the GFAP-Cre-IRES-LacZ transgene, and 0.5 μg of the original GFAP-Cre-IRES-LacZ *Bgl*II/*Not*I fragment used for pronuclear injection were separated by 1% agarose gel electrophoresis, followed by capillary transfer onto Hybond-N nylon membranes (Amersham, Piscataway, N.J.). The *Hin*dIII Cre fragment (≈1 kb) of the PSA-Cre-HGH construct was labeled with [α-^{32}P]dATP by using the Prime-a-gene labeling system (Promega, Madison, Wis.). The ^{32}P-radiolabeled Cre-purified probe was hybridized to the membranes at 42°C overnight, washed three times in 2× SSC (1× SSC is 0.15 M NaCl plus 0.015 M sodium citrate)–0.1% sodium dodecyl sulfate (SDS) at 60°C, and exposed at −80°C for 48 h. Three founders were identified by PCR and Southern blotting and bred with C57BL/6 mice to generate three transgenic lines (1, 6, and 8).

To establish astrocyte-specific *Nf1* knockout mice, each of the three GFAP-Cre lines was crossed with the *Nf1flox/flox* mice, containing LoxP sites flanking exons 31 and 32 of the *Nf1* gene. The *Nf1flox/flox* mice were genotyped, and recombination PCR was performed with specific primers able to recognize only the recombined *Nf1* gene (48).

$Nf1^{+/-}$ mice were generously provided by Neal Copeland (National Institutes of Health) (8). All mouse strains are maintained as permanent colonies in the Department of Comparative Medicine small-animal barrier facility at the Washington University School of Medicine.

Staged embryos for LacZ reporter expression analysis were generated by breeding GFAP-Cre transgenic mice with C57BL/6 mice, while embryonic E12.5 $Nf1^{-/-}$ astrocyte cultures were generated by interbreeding $Nf1^{+/-}$ mice, with the assignment of noon on the day after the appearance of a mucous plug in mated animals as embryonic day 0.5 (E0.5).

Tissue preparation for histological analysis. For β-galactosidase activity and/or immunohistochemistry of brain sections, mice were perfused transcardially with 0.1 M sodium phosphate buffer, pH 7.4, followed by 4% paraformaldehyde in 0.1 M sodium phosphate buffer, pH 7.4. The brains were removed and fixed by immersion in 4% paraformaldehyde in 0.1 M phosphate buffer overnight at 4°C. After fixation, the brains were cryoprotected in 30% sucrose solution in 0.1 M phosphate buffer at 4°C. For microtome sections, the cryopreserved brains were frozen in powdered dry ice. Tissue sections were then cut in the coronal plane at 40 μm on a freezing sliding MICROM HM 400 microtome (Microme GmbH, Berlin, Germany).

For β-galactosidase activity staining, staged embryos were removed in cold 0.1 M phosphate buffer (pH 7.4) and fixed in 4% paraformaldehyde in 0.1 M phosphate buffer for 24 h at 4°C. Whole 11.5- and 13.5-day-old embryos and bisected 14.5-, 15.5-, and 18.5-day-old embryos were rinsed with phosphate-buffered saline (PBS) buffer (pH 7.3) prior to 5-bromo-4-chloro-3-indolyl-β-D-galactopyranoside (X-Gal) staining.

For hematoxylin and eosin staining, GFAP immunohistochemistry, PCNA/GFAP and LacZ/Cre double immunofluorescence of brain sections, and S-100 staining of sciatic nerve sections, brains and sciatic nerves of the $Nf1^{GFAP}CKO$ as well as control *Nf1flox/flox* and *Nf1flox/wt* mice were removed, washed with PBS, and fixed overnight in Bouin's fixative (15 parts saturated picric acid, 5 parts 37% formaldehyde, 1 part glacial acetic acid; Sigma, St. Louis, Mo.). The brains and sciatic nerves were washed in 70% ethanol and submitted in 70% ethanol to the Washington University Molecular Biology and Pharmacology Histology Core Facility for paraffin embedding and sectioning.

Immunostaining and astrocyte counting. GFAP was employed as a marker for mature differentiated astrocytes in the brain, while adenomatous polyposis coli (APC), microtubule-associated protein 2 (MAP2), and S-100 were used as protein markers for oligodendrocytes, neurons, and Schwann cells, respectively. Free-floating sections (40 μm) were processed for immunohistochemistry by using a rat monoclonal anti-GFAP antibody (1:10,000 dilution; Zymed, San Francisco, Calif.), a mouse monoclonal anti-APC antibody (1:500 dilution; Oncogene, Cambridge, Mass.), and a mouse monoclonal anti-MAP2 antibody (1:500 dilution; PharMingen, San Diego, Calif.), respectively. Sciatic nerve paraffin sections (4 μm) were processed for S-100 staining with a polyclonal anti-S-100 antibody (1:50,000 dilution; Z311, Dako, Carpinteria, Calif.). Cre immunostaining was performed on 40-μm free-floating sections with a polyclonal anti-Cre antibody (1:60,000 dilution; Novagen, Madison, Wis.).

Brain sections were then incubated with biotinylated secondary antibodies

(1:1,000 dilution) and detected with the Vectastain ABC Elite kit (Vector Laboratories, Burlingame, Calif.). The substrate for the horseradish peroxidase color reaction was diaminobenzidine (DAB; brown reaction product). For combined immunohistochemistry and β-galactosidase staining, brain sections from 7- to 14-day-old GFAP-Cre transgenic mice were first processed for GFAP, APC, or MAP2 immunohistochemistry followed by LacZ histochemistry. β-Galactosidase staining was performed by incubating the brain sections for several hours to overnight at 37°C in PBS buffer (pH 7.3) containing 2 mM $MgCl_2$, 0.02% NP 40, 0.01% sodium deoxycholate, 5 mM potassium ferrocyanide, 5 mM potassium ferricyanide, and 1 mg of X-Gal per ml. Sections were mounted on slides with Cytoseal-60 mounting medium for microscopy (Stephens Scientific, Kalamazoo, Mich.) and photographed with a digital camera (Optronics) attached to an inverted microscope (Nikon).

To analyze LacZ expression during embryonic development of GFAP-Cre transgenic mice, staged embryos were stained as above for brain sections. After several rinses with PBS (pH 7.3), embryos were photographed with a digital camera (Optronics) attached to a dissection microscope (Nikon).

GFAP-immunoreactive astrocytes were counted in the CA1 region of the hippocampus of brain sections from adult and 2-, 6-, and 12-month-old *Nf1*^{GFAP}*CKO* mice and control mice (18, 37). Two-month-old GFAP-Cre and *Nf1flox/flox* mice and 6- and 12-month-old *Nf1flox/flox* and *Nf1flox/wt* mice were used as controls. Astrocytes were counted in six consecutive serial sections per brain obtained from four to six animals of each genotype. Data are presented as means ± standard deviations (SD) and were analyzed with analysis of variance followed by the Bonferoni T test, with significance set at $P < 0.05$.

Hematoxylin and eosin staining was performed according to standard protocols.

PCNA/GFAP and Cre/LacZ double immunofluorescence. For tyramide signal amplification enhanced immunohistochemical detection (46), 4-μm paraffin sections were first subjected to deparaffinization in Citrisolv (Fisher Scientific) and then incubated overnight at 4°C with primary antibodies: for PCNA, goat polyclonal anti-PCNA antibody (C20) (1:800 dilution; Santa Cruz); for GFAP, a rat monoclonal anti-GFAP antibody (1:100 dilution; Zymed, San Francisco, Calif.); for Cre, a rabbit polyclonal antibody (1:6,000; Novagen, Madison, Wis.); and for LacZ, a mouse monoclonal antibody (1:500; Oncogene, Boston, Mass.). Secondary horse anti-goat (Vector Laboratories, Burlingame, Calif.; 1:1,000), rabbit anti-rat (Sigma; 1:1,000), goat anti-mouse (Sigma; 1:1,000), and goat anti-rabbit (Sigma; 1:2,000) antibodies were used. TSA-Plus fluorescein and cyanin 3 system kits (Perkin-Elmer Life Sciences, Inc., Boston, Mass.) were used for fluorescence detection by following the manufacturer's directions. Sections were mounted in Vectashield mounting medium for fluorescence with DAPI (4′,6′-diamidino-2-phenylindole) (Vector Laboratories, Burlingame, Calif.). DAPI was used to counterstain DNA and identify cell nuclei in the sections.

Primary astrocyte cultures. Murine neocortical astrocyte cultures were established from postnatal day 2 pups as previously described (3, 21). E12.5 astrocyte cultures were generated from the forebrains of 12.5-day-old embryos removed from euthanized *Nf1*$^{+/-}$ timed-pregnancy mothers. Genotypes were determined by PCR from tail DNA.

Astrocyte proliferation in culture was determined by direct counting or thymidine incorporation. For direct counting, 10^5 cells were seeded, harvested after 3 and 6 days in culture (1, 3, and 5 days), and counted by using a Hausser Scientific hemacytometer. [^{3}H]thymidine incorporation was performed as previously reported (18).

Cell cycle analysis of cultured astrocytes was performed by measuring the cellular DNA content by flow cytometry, according to established protocols (36). Briefly, 10^5 cells were seeded in 100-mm culture dishes maintained in growth medium with 10% horse serum and harvested at 75% confluency for flow cytometry of the DNA content. The cells were washed with PBS and fixed in 70% ethanol. Immediately prior to the flow cytometry analysis, cells were stained with freshly prepared propidium iodide solution containing RNase A for 30 min at 37°C, and 10,000 cells were analyzed for each sample on a FACSCalibur (Becton Dickinson) flow cytometer. Cell cycle analysis was performed three times with identical results.

Anchorage-independent growth was determined by using established techniques. Briefly, 2,500 cells in 0.3% Noble agar were seeded in quadruplicate wells of a 24-well plate, and the number of colonies was determined by direct counting after 2 to 3 weeks. Rat C6 glioma cells were used as a positive control.

Cre-adenovirus and LacZ-adenovirus infection of primary cultured astrocytes. Primary astrocyte cultures were prepared from the brains of postnatal day 2 *Nf1flox/flox* mice as described above. Adenovirus type 5 (Ad5)-Cre and Ad5-LacZ were purchased from the University of Iowa Gene Transfer Vector Core (B. Davidson, Iowa City, Iowa). Briefly, *Nf1flox/flox* astrocytes at 75 to 80% confluency were treated with Ad5-Cre or control Ad5-LacZ virus diluted in growth medium containing 10% horse serum at a multiplicity of infection of 50 for 1 h at 37°C. After 1 h, the medium was removed, and the infected *Nf1flox/flox* astrocytes were washed with PBS, pH 7.4, and then maintained in growth medium with 10% horse serum for 4 days. We experimentally determined that 4 days represented the optimal time for complete *Nf1* gene recombination and loss of neurofibromin expression. After 4 days in culture, the Ad5-Cre- and Ad5-LacZ-infected *Nf1flox/flox* astrocytes were collected for Western blotting or proliferation assays, anchorage-independent growth experiments, or intracranial implantation in immunocompromised (*nu/nu*) mice.

Intracranial implantation of astrocytes in nude mice. A total of 8×10^5 E12.5 *Nf1*$^{-/-}$ and *Nf1*$^{+/+}$ astroglial cells or *Nf1*$^{-/-}$ astrocytes and *Nf1*$^{+/+}$ astrocytes generated by Ad5-Cre and Ad5-LacZ infection of *Nf1flox/flox* astrocytes were resuspended in 10 μl of growth medium and injected intracranially under aseptic conditions into the brains of 6- to 8-week-old anesthetized athymic *nu/nu* mice by using a stereotactic injection apparatus. The injection hole was filled with bone wax, the skin was closed with staples, and injected mice were returned to their cages for 8 to 12 weeks. Mice were euthanized, and their brains were removed for processing and paraffin embedding.

Western blot analysis. Western blot analysis was performed on cultured astrocyte extracts prepared by homogenization in lysis buffer (20 mM Tris [pH 7.5], 150 mM NaCl, 1 mM EDTA, 1 mM EGTA, 1% Triton X-100, 2.5 mM sodium pyrophosphate, 1 mM glycerophosphate, 1 mM sodium orthovanadate, 1 ng of leupeptin per ml). Protein concentrations were determined by using the BCA protein assay (Pierce Chemical Company). Proteins were separated by sodium dodecyl sulfate-polyacrylamide gel electrophoresis (SDS-PAGE) and transferred onto Immobilon membranes (Millipore) for Western blotting. WA15a neurofibromin (17) or NF1GRP-D (Santa Cruz Biotechnology Inc., Santa Cruz, Calif.) (1:300 dilution) and tubulin antibodies (1:20,000 dilution; mouse monoclonal DM1A; Sigma, St. Louis, Mo.) were used as primary antibodies. Secondary antibodies were horseradish peroxidase-conjugated reagents (Sigma). Detection was performed by using ECL chemiluminescence (Amersham).

RESULTS

Generation and characterization of GFAP-Cre transgenic mice. To achieve astrocyte-specific Cre-mediated excision of the *Nf1* gene, we generated several lines of mice expressing Cre recombinase under the control of the human GFAP promoter. The 2.2-kb fragment of the human GFAP promoter (Gfa2) was chosen based on previous work by Messing and Brenner demonstrating astrocyte-specific expression in transgenic mice (9). The IRES sequence was inserted to allow for cotranslation of the nucleus-targeted Cre and β-galactosidase (LacZ) proteins from the same mRNA (Fig. 1A). In this fashion, LacZ

FIG. 1. Generation and characterization of GFAP-Cre transgenic mice. (A) Schematic diagram of the GFAP-Cre-IRES-LacZ transgene. The transgene contains the 2.2-kb fragment of the human GFAP promoter (hGFAP) and cDNAs encoding the nucleus-targeted proteins Cre recombinase (Cre) and β-galactosidase (nLacZ). The IRES sequence allows cotranslation of the Cre and LacZ proteins from the same mRNA. (B) Southern blot analysis of DNA from mouse tail biopsies digested with *Bgl*II and *Not*I to excise the GFAP-Cre-IRES-LacZ transgene (first five lanes) and of the original GFAP-Cre-IRES-LacZ construct used for pronuclear injection (lane +) with a 1-kb Cre probe. Founder 8 carries an 8-kb transgene identical to the original construct (lane +). The GFAP-Cre transgenic mice showed strong LacZ expression in the brain (C), while no LacZ expression was observed in the brain of wild-type littermates (D). Cre immunohistochemistry demonstrated Cre expression in the CA1 region of the hippocampus of the GFAP-Cre mice (E), whereas no Cre expression was detected in wild-type littermates (F). Double immunofluorescence with anti-β-galactosidase antibodies (H; green) and anti-Cre antibodies (I; red) demonstrated colocalization of the Cre and LacZ nuclear protein expression in the same cells in the CA1 region of the hippocampus (J; yellow). DAPI staining of nuclei is shown in panel G.

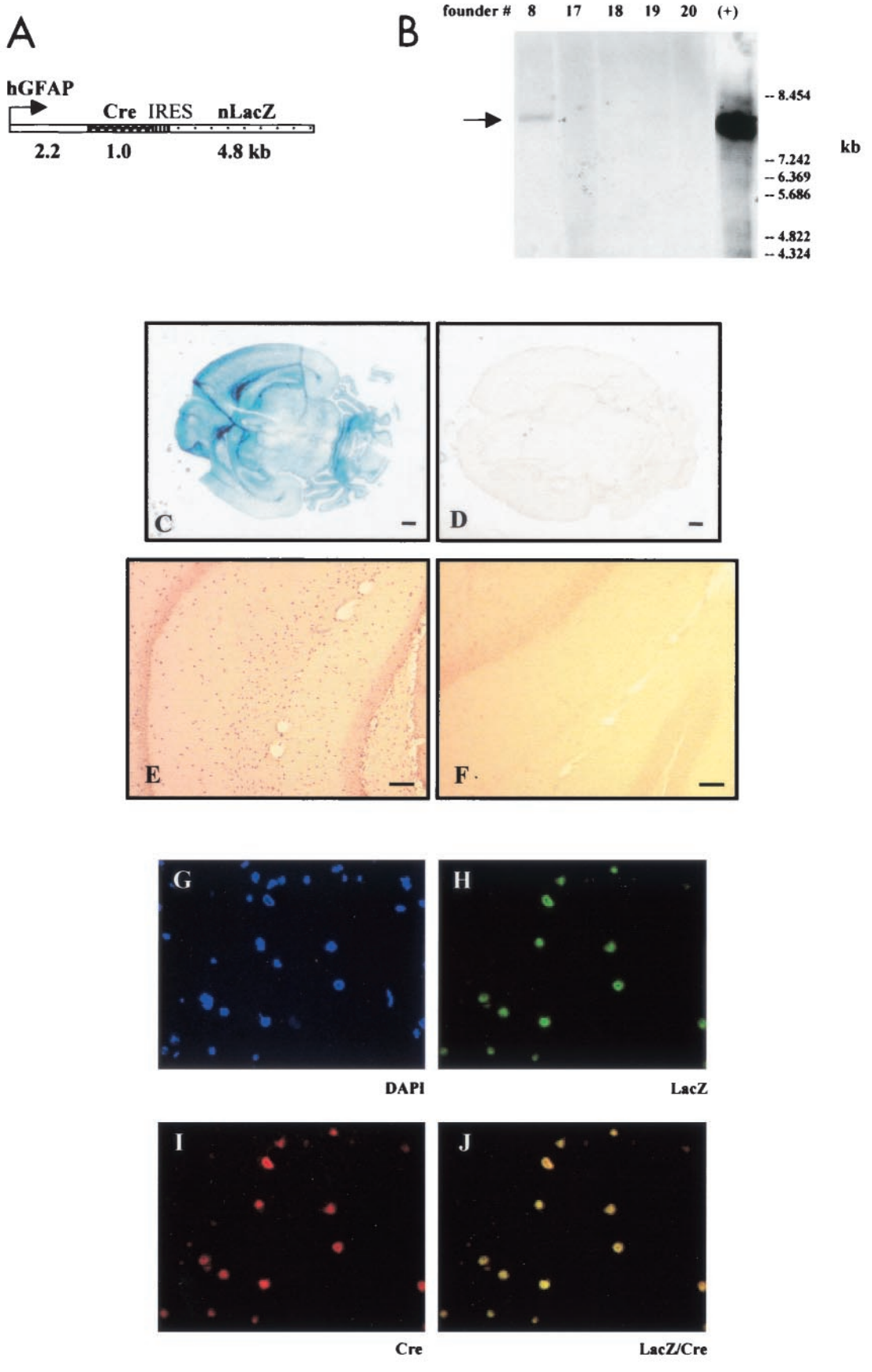
A
hGFAP
Cre IRES nLacZ
2.2
1.0
4.8 kb
B
founder # 8 17 18 19 20 (+)
-- 8.454
-- 7.242
-- 6.369
-- 5.686
-- 4.822
-- 4.324
kb
C
D
E
F
G
H
DAPI
LacZ
I
J
Cre
LacZ/Cre

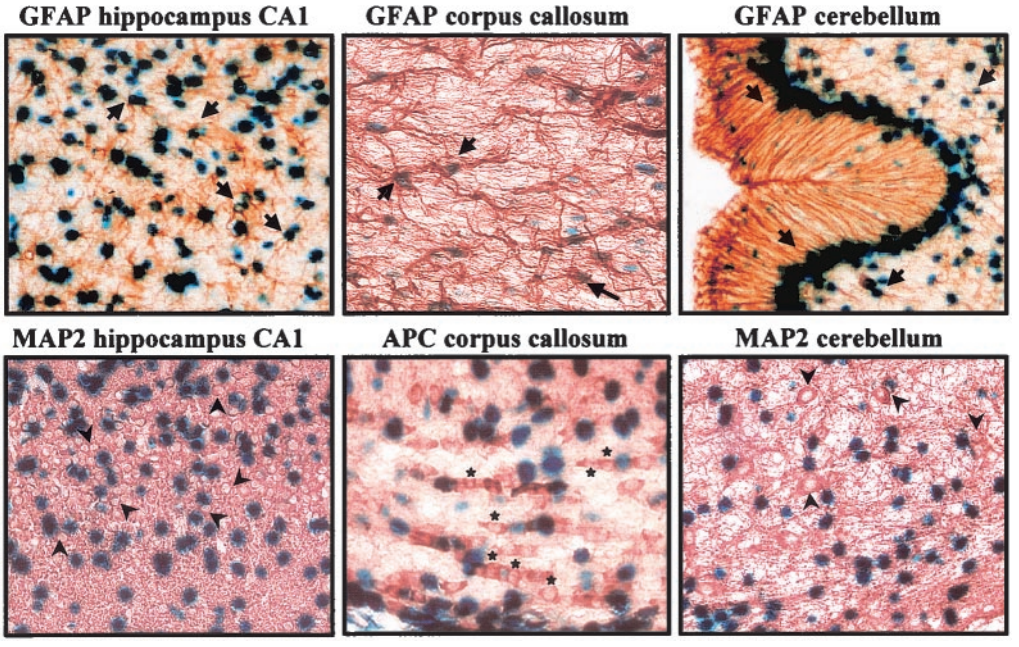

FIG. 2. β-Galactosidase is expressed only in astrocytes in the brains of GFAP-Cre mice. LacZ is specifically expressed in GFAP-immunoreactive astrocytes (arrows point to representative astrocytes expressing LacZ) in the hippocampus, corpus callosum, and cerebellum. Note that Bergmann glia in the cerebellum show high LacZ expression. APC-immunoreactive oligodendrocytes (stars) in the corpus callosum and MAP2-immunoreactive neurons (arrowheads denote the neuronal cell bodies) in the hippocampus and cerebellum of the GFAP-Cre transgenic mice do not demonstrate LacZ activity. Magnification, ×400.

reporter activity represents an indirect but reliable method for detecting Cre expression patterns in vivo and facilitates the identification of *Nf1*$^{-/-}$ astrocytes.

We identified three founders by genotyping with Cre- and LacZ-specific primers (lines 1, 6, and 8). Southern blotting of tail DNA with a ^{32}P-radiolabeled Cre probe verified the PCR results (Fig. 1B). Founders were then crossed onto the C57BL/6 background, and their offspring were evaluated for β-galactosidase activity in sections of several organs from 7-day-old transgenic pups. Robust LacZ expression was detected in the brain (Fig. 1C) but not in other organs, including heart, liver, kidney, and intestine (data not shown). No LacZ expression was detected in wild-type littermates (Fig. 1D). High levels of Cre expression were similarly detected in the brains of GFAP-Cre transgenic mice (Fig. 1E), whereas no expression was observed in control littermates (Fig. 1F). Double immunofluorescence with anti-β-galactosidase and anti-Cre antibodies showed that the Cre and LacZ expression colocalized in the nuclei of the same cells in GFAP-Cre transgenic mice (Fig. 1H, I, and J). There was neither LacZ nor Cre immunofluorescence in brain sections from wild-type littermates (not shown).

To evaluate the astrocyte specificity of LacZ expression in these GFAP-Cre transgenic mice, we performed immunohistochemistry by using antibodies that identify astrocytes, oligodendrocytes, and neurons in combination with X-Gal staining. LacZ expression was found in GFAP-positive astrocytes in most regions of the brain, including hippocampus, corpus callosum, and cerebellum, but not in MAP2-positive neurons or APC-positive oligodendrocytes (Fig. 2). Similarly, no LacZ expression was found in S-100-positive Schwann cells, associated with either large myelinated axons or small unmyelinated axons, in the sciatic nerve (data not shown).

Two lines of transgenic mice were selected for further analysis (lines 1 and 8), and the results from one line (line 8) are presented in this paper. Identical results were obtained with line 1.

To determine when GFAP promoter-directed transgene expression was first detected in these lines, we performed a developmental profile of β-galactosidase activity during mouse embryogenesis. β-Galactosidase activity was first detected by embryonic day 14.5 in both transgenic lines. By embryonic day 18.5, LacZ was robustly expressed in the brain, spinal cord, and optic nerves of GFAP-Cre transgenic animals (Fig. 3).

To assess the function of the Cre transgene, GFAP-Cre mice were crossed with the Z/AP reporter mouse strain (32). Efficient Cre-mediated recombination resulted in loss of cytoplasmic β-galactosidase activity and expression of the human alkaline phosphatase gene in astrocytes in the brain in vivo (A. Guha, unpublished observations). Thus, these GFAP-Cre-IRES-LacZ transgenic mice represent an efficient and specific tool to delete conditional LoxP-interrupted genes specifically in astrocytes in the mouse nervous system.

***Nf1* astrocyte-specific knockout mice (*Nf1*^{GFAP}*CKO*) do not develop astrocytomas.** To establish an astrocyte-specific *Nf1* knockout mouse, we successively crossed GFAP-Cre-IRES-LacZ mice with *Nf1flox/flox* mice. *Nf1flox/flox* mice have two functional *Nf1* alleles containing *loxP* sequences, as previously reported (48). The *Nf1flox* allele behaves like a wild-type allele despite the presence of an intronic neomycin resistance cassette and *loxP* sequences. *Nf1flox/flox* mice have been breeding for several years in our colony as well as in Parada's laboratory

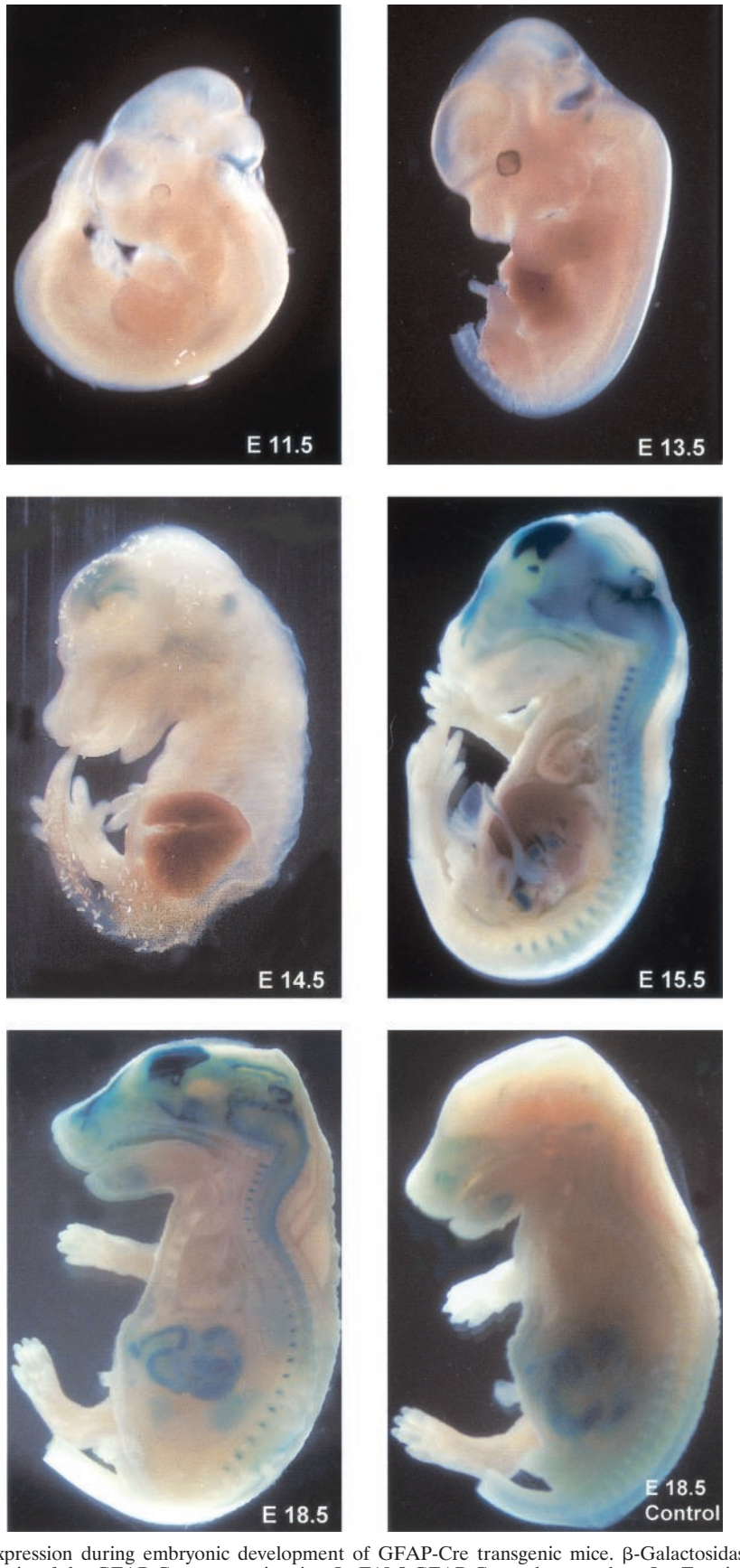

FIG. 3. LacZ reporter expression during embryonic development of GFAP-Cre transgenic mice. β-Galactosidase activity was detected by embryonic day 14.5 in the brain of the GFAP-Cre transgenic mice. In E18.5 GFAP-Cre embryos, robust LacZ activity is detected in the brain, spinal cord, and optic nerves. No LacZ expression is observed in a control littermate (E18.5 control). The intestines of both GFAP-Cre and control mice show endogenous LacZ activity. Mouse embryos were photographed at ×8 magnification at E11.5 and E13.5, ×5 magnification at E15.5, and ×3 magnification at E18.5.

without evidence of neurological or brain anatomical abnormalities.

A cohort of 40 *Nf1*^{GFAP}*CKO* mice and control littermates (*Nf1flox/flox* and *Nf1flox/wt* mice) were monitored for 20 months for gross neurological abnormalities. These mice did not show differences in size or weight compared to control littermates and they were healthy and fertile. Hematoxylin and eosin staining of their brains did not reveal any astrocytomas. Analysis of serial coronal brain sections from 10- to 12-month-old *Nf1*^{GFAP}*CKO* mice ($n = 9$) and control littermates ($n = 9$) did not identify any abnormalities suggestive of astrocytomas. Finally, we were not able to detect any tumors by T1- and T2-weighted magnetic resonance imaging by using a brain and optic nerve protocol in 12-month-old *Nf1*^{GFAP}*CKO* mice ($n = 2$) (S.-K. Song, data not shown).

***Nf1*^{GFAP}*CKO* mice exhibit increased numbers of astrocytes throughout the brain.** Histological analysis of brain sections by immunohistochemistry with the GFAP antibody revealed moderate increases in astrocyte numbers throughout the brains of *Nf1*^{GFAP}*CKO* mice. In Fig. 4, whole brain sections, aligned from rostral to caudal, showed higher GFAP staining in *Nf1*^{GFAP}*CKO* mice (right side of the panels, CKO) than brain sections from control mice (left side of the panels, C). We did not observe any reproducible regional differences in astrocyte numbers, and the increased astrocytes appeared to be uniformly distributed throughout the brain. Higher magnification identified increased numbers of astrocytes in several brain regions, including the corpus callosum, cerebral cortex, and hippocampus, of the conditional knockout mice (Fig. 4a to f).

To better analyze the morphology of the astrocytes, we also performed GFAP and eosin staining of thin paraffin coronal sections of the brains of adult *Nf1*^{GFAP}*CKO* mice. Although we observed a higher number of GFAP-immunoreactive astrocytes in the dentate gyrus as well as the CA1/CA2 and CA3 areas of the hippocampus in *Nf1*^{GFAP}*CKO* mice than in their control littermates, the morphology of the GFAP-positive astrocytes was similar between the mutant and the control mice (Fig. 4g to l).

The number of astrocytes was determined by counting the GFAP-immunoreactive cells (astrocytes) in the CA1 region of the hippocampus of mutant mice and control mice. As shown in Fig. 5A, 1.6-fold more astrocytes were present in the CA1 region of the hippocampus of 2-month-old *Nf1*^{GFAP}*CKO* ($n = 4$) mice compared with control littermates (*Nf1flox/flox* [$n = 4$] and *GFAP-Cre* mice [$n = 4$]). The number of astrocytes in the CA1 region of the *Nf1*^{GFAP}*CKO* mice increased slightly in older mutant mice, rising to 1.8-fold at 6 months of age ($n = 3$) and 2.2-fold at 12 months ($n = 5$) (Fig. 5B and C). The 6- and 12-month-old control mice were either *Nf1flox/flox* or *Nf1flox/wt* littermates.

To assess whether the increased number of GFAP-positive astrocytes in the brain resulted from increased glial fibrillary acidic protein expression, a property of reactive astrocytes, or increased astrocyte proliferation, we performed double immunofluorescence with anti-GFAP and anti-PCNA (proliferating cell nuclear antigen) antibodies in coronal brain sections from adult *Nf1*^{GFAP} *CKO* mutant mice ($n = 3$) and control mice ($n = 3$). There were increased numbers of PCNA-labeled cells in the hippocampus (dentate gyrus as well as the CA1 and CA2/CA3 regions) of *Nf1*^{GFAP}*CKO* mice compared to control mice (Fig. 6a), and 75% of the PCNA-positive (proliferating) cells were GFAP immunoreactive and exhibited typical astrocyte morphology, whereas 25% of the PCNA-labeled cells were GFAP negative (Fig. 6c). We believe that these PCNA-labeled cells represent astrocytes (GFAP positive) and astroglial precursor cells (GFAP negative) at different stages of development. Since PCNA is a marker for proliferating cells, we conclude that the increased number of astrocytes observed in our *Nf1*^{GFAP}*CKO* mice reflects an increase in astrocyte proliferation.

Loss of *Nf1* affects the growth but not the tumorigenic properties of *Nf1*^{GFAP}*CKO* astrocytes in vitro. Analysis of primary astrocyte cultures derived from *Nf1* conditional knockout mice demonstrated efficient Cre-mediated excision of the *Nf1* gene by PCR with primer sets that specifically recognize the recombined *Nf1* allele *(R-Nf1)*. Whereas the PCR *Nf1* recombination product was present in both GFAP-Cre *Nf1flox/flox (Nf1*^{GFAP}*CKO)* and GFAP-Cre *Nf1flox/wt* astrocytes, no recombination was detected in astrocyte cultures derived from *Nf1flox/flox* littermates lacking Cre (Fig. 7A). As shown in Fig. 7B, neurofibromin expression was absent in astrocytes derived from GFAP-Cre *Nf1flox/flox* (*Nf1*^{GFAP}*CKO*) mice, and protein levels were significantly decreased in GFAP-Cre *Nf1flox/wt* astrocytes compared to *Nf1flox/flox* astrocytes lacking Cre, as determined by Western blotting with a neurofibromin-specific antibody. Tubulin was included as a control for protein loading.

We have previously demonstrated that heterozygosity for *Nf1* confers a growth advantage for astrocytes in vitro and in vivo (3, 18). To examine the role of neurofibromin in astrocyte growth and tumor formation, we analyzed the growth and tumorigenic properties of primary cultured astrocytes derived from 2-day-old *Nf1*^{GFAP}*CKO* and control *Nf1flox/flox* mice. When astrocytes in culture at passage 1 were harvested and counted, we observed a twofold growth advantage for *Nf1*^{GFAP}*CKO* compared with *Nf1flox/flox* astrocytes, as shown in Fig. 7C. These results were also observed by [^{3}H]thymidine incorporation and flow cytometry analysis of the cellular DNA content (data not shown). Although neurofibromin loss enhanced the growth properties of *Nf1*^{GFAP}*CKO* astrocytes, *Nf1* null astrocytes lacked tumorigenic properties. The astrocytes derived from these *Nf1* astrocyte-specific conditional knockout mice did not grow in serum-free medium and were not able to form colonies in soft agar (data not shown).

***Nf1* inactivation influences the growth but not the tumorigenic properties of embryonic or postnatal *Nf1*$^{-/-}$ astroglial cells.** Our developmental study of β-galactosidase activity in the GFAP-Cre transgenic mice indicates that Cre-mediated disruption of the *Nf1* gene in astrocytes likely begins around embryonic day 14.5. To eliminate the possibility that tumor formation requires *Nf1* inactivation at a different developmental time than embryonic day 14.5, we established embryonic astroglial cultures from brains of conventional *Nf1* knockout mice (*Nf1*$^{-/-}$) at embryonic day 12.5 and deleted the *Nf1* gene in astrocytes in vitro derived from postnatal day 2 *Nf1flox/flox* mice by adenovirus-mediated Cre delivery.

Since conventional *Nf1*$^{-/-}$ mice die in utero between embryonic days 12.5 and 14 of a heart developmental defect (double outlet right ventricle), we prepared primary astroglial cultures from the brains of *Nf1*$^{-/-}$ mice at embryonic day 12.5.

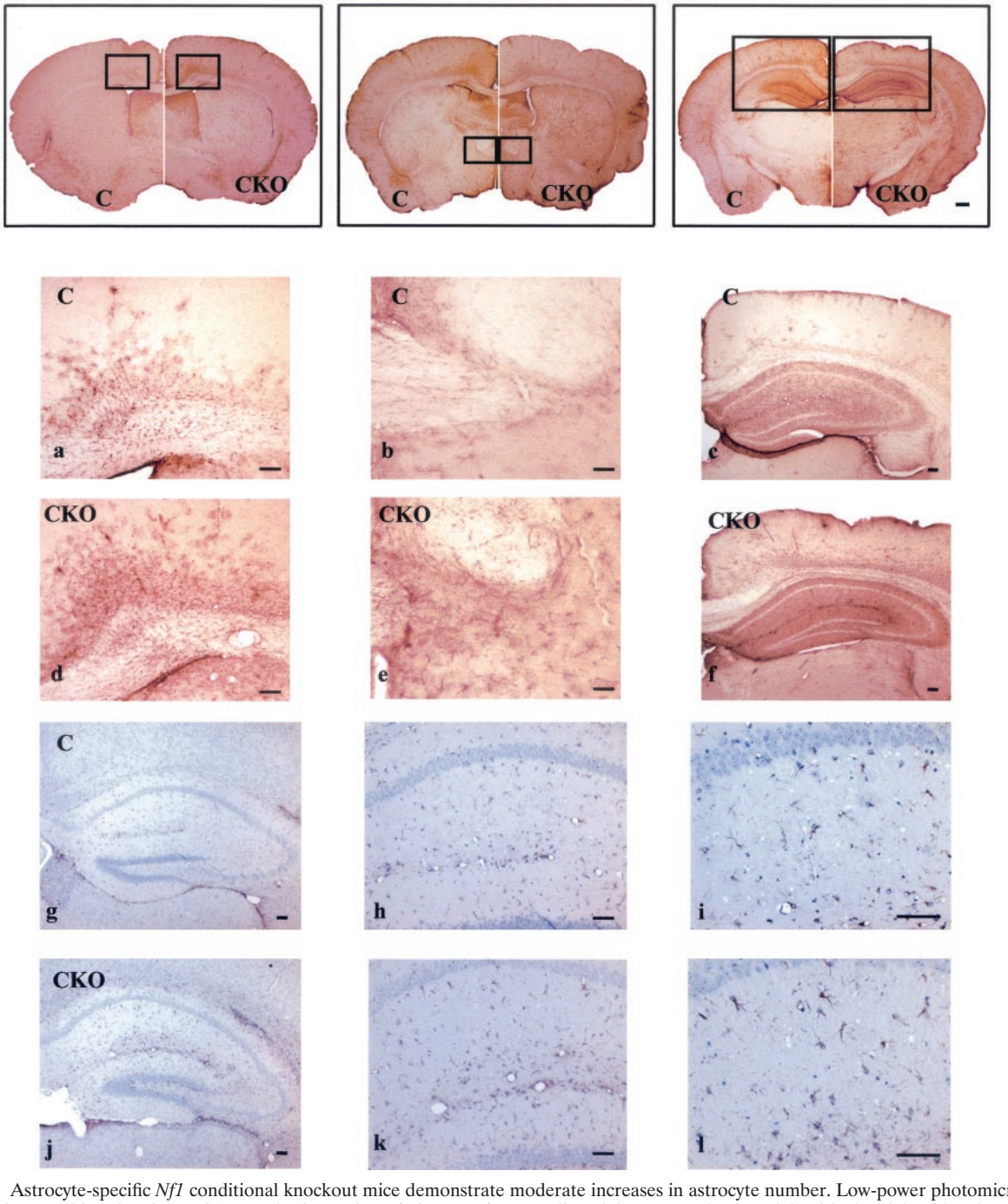

FIG. 4. Astrocyte-specific *Nf1* conditional knockout mice demonstrate moderate increases in astrocyte number. Low-power photomicrographs of GFAP immunohistochemistry of 40-μm brain sections (microtome) were aligned from rostral to caudal, with the right side of each panel representing $Nf1^{GFAP}CKO$ brain sections (CKO) and the left side of each panel representing brain sections from control mice (C). $Nf1^{GFAP}CKO$ mice demonstrate increased GFAP immunoreactivity throughout the brain. Higher magnification of the boxed areas in the brains of control mice (C) on the left side of the upper panels (a, b, and c) and of the boxed areas in the brains of $Nf1^{GFAP}CKO$ mice (CKO) on the right side of the upper panels (d, e, and f) revealed increased numbers of astrocytes in the corpus callosum, hippocampus, and cortex of $Nf1^{GFAP}CKO$ mice. Increased numbers of astrocytes without major changes in morphology were also observed in $Nf1^{GFAP}CKO$ hippocampal sections by GFAP and eosin staining (panels j, k, and l) compared to control mice (panels g, h, and i).

Immunofluorescence analysis of $Nf1^{-/-}$ astroglial cells in culture with anti-GFAP and antinestin antibodies, a marker for undifferentiated neural cells, revealed that most of the cells in culture (90%) were GFAP positive, while only a few of the cells (10%) were nestin positive and GFAP negative. $Nf1^{-/-}$ astroglial cells exhibited a slightly different morphology than their $Nf1^{+/-}$ and wild-type counterparts: they were smaller in size, had a more elongated shape, and extended fewer processes (data not shown). Western blotting of cellular extracts from the cultured astroglial cells confirmed the loss of neuro-

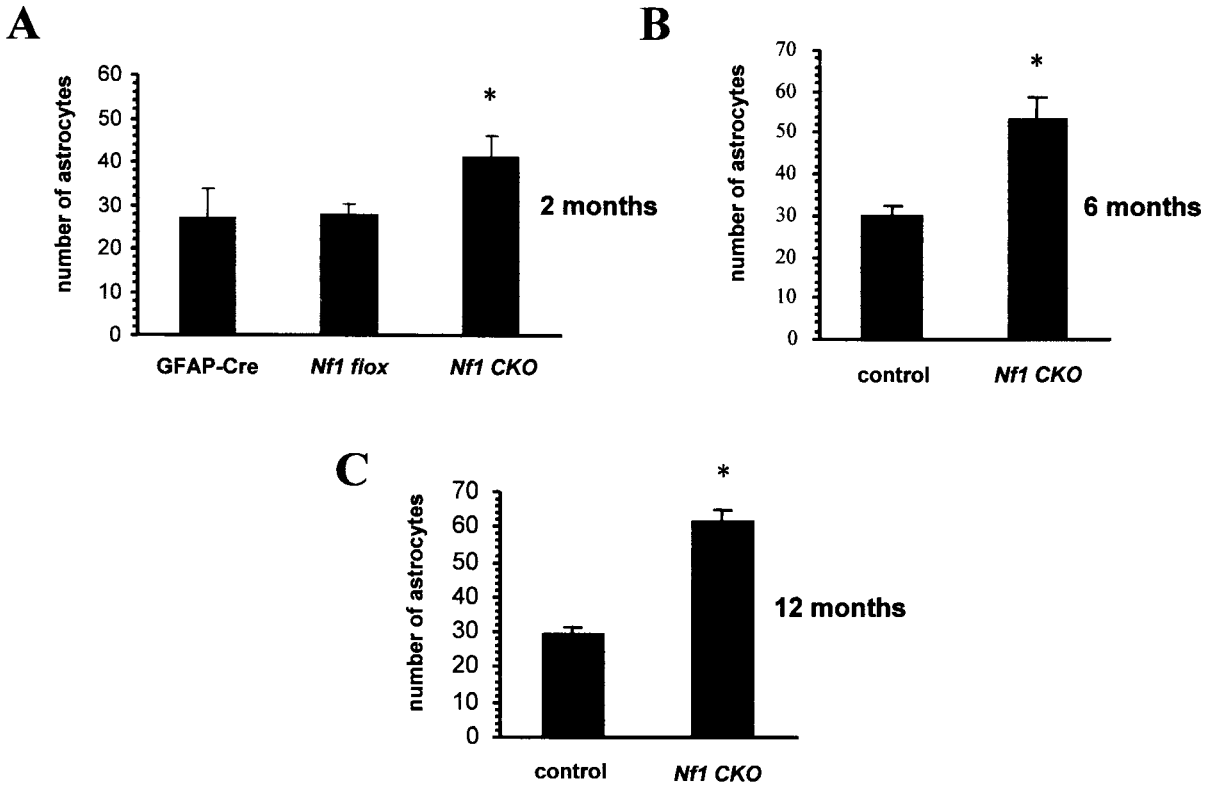

FIG. 5. The number of GFAP-immunoreactive astrocytes is increased in the hippocampus CA1 region of astrocyte-specific *Nf1* conditional knockout mice compared to that of control littermates. Quantitation of the GFAP-positive astrocytes in the CA1 region of the hippocampus of the mutant and control mice demonstrated 1.6-fold more astrocytes in 2-month-old $Nf1^{GFAP}CKO$ mice than in GFAP-Cre and *Nf1flox/flox* controls (A) and a slight increase to 1.8-fold in 6-month-old (B) and to 2.2-fold in 12-month-old (C) $Nf1^{GFAP}CKO$ mice compared with *Nf1flox/flox* and *Nf1flox/wt* controls. Data are presented as mean values ± SD and were analyzed by analysis of variance followed by the Bonferroni *t* test, with significance set at $P < 0.05$.

fibromin in $Nf1^{-/-}$ cells, whereas the $Nf1^{+/-}$ cells had approximately half of the amount of neurofibromin present in wild-type astrocytes (Fig. 8A).

Nf1 null embryonic astrocytes demonstrated a fourfold increase in growth compared to $Nf1^{+/+}$ and a twofold increase in growth compared to $Nf1^{+/-}$ astrocytes (Fig. 8B). These results were confirmed by [^{3}H]thymidine incorporation (Fig. 8C) and flow cytometry analysis of the cell cycle (Fig. 8D). In these experiments, 77.5%, 9.6%, and 13.19% of the $Nf1^{+/-}$ astroglial cells were in G_1, S, and G_2/M, respectively, whereas 55.9%, 22.84%, and 22.07% of the $Nf1^{-/-}$ astroglial cells were in G_1, S, and G_2/M, respectively. However, $Nf1^{-/-}$ astroglial cells did not grow in serum-free medium and did not form colonies in soft agar (Fig. 8E). In addition, embryonic day 12.5 astroglial $Nf1^{-/-}$ cells were not able to induce astrocytoma formation after intracranial implantation in the brains of immunocompromised, athymic (*nu*/*nu*) mice (data not shown; $n = 3$).

To disrupt *Nf1* at a later developmental time, we used high-titer replication-defective adenoviruses containing Cre recombinase (Ad5-Cre) or β-galactosidase (Ad5-LacZ) under the control of the human cytomegalovirus promoter (41). Viral delivery of Cre or LacZ (control) was achieved by infecting astrocyte cultures derived from *Nf1flox/flox* cortex at postnatal day 2 with Ad5-Cre and Ad5-LacZ (2). Complete Cre-mediated recombination of the *Nf1* gene was achieved at a multiplicity of infection of 50 and verified at the DNA level by PCR analysis with specific primers (Fig. 9A) and at the protein expression level by Western blotting (Fig. 9B).

Cre- and LacZ-adenovirus-infected *Nf1flox/flox* astrocyte cultures (multiplicity of infection = 50) were monitored for their growth properties. The astrocytes infected with the Cre-adenovirus exhibited a 1.7-fold growth advantage over the LacZ-adenovirus-infected astrocytes after 5 days in culture (Fig. 9C). In addition, loss of *Nf1* expression at a later time in the development of astrocytes did not confer any tumorigenic properties on these astrocytes. Cre-infected *Nf1flox/flox* astrocytes did not grow in serum-free medium, did not form colonies in soft agar, and were not able to induce astrocytomas when injected in the brains of immunocompromised (*nu*/*nu*) mice ($n = 3$) (data not shown).

DISCUSSION

Previous studies have suggested that the *Nf1* gene product, neurofibromin, is an important growth regulator for astrocytes. First, reduced *Nf1* gene expression is associated with increased astrocyte proliferation in vivo and in vitro (3, 18). This heterozygous growth advantage is cell autonomous and is associated with increased $p21^{ras}$ pathway activation, consistent with the function of neurofibromin as a $p21^{ras}$-GAP. Second, neurofibromin expression increased during astrocyte growth arrest under physiologic conditions in vitro (18, 21). Third, individu-

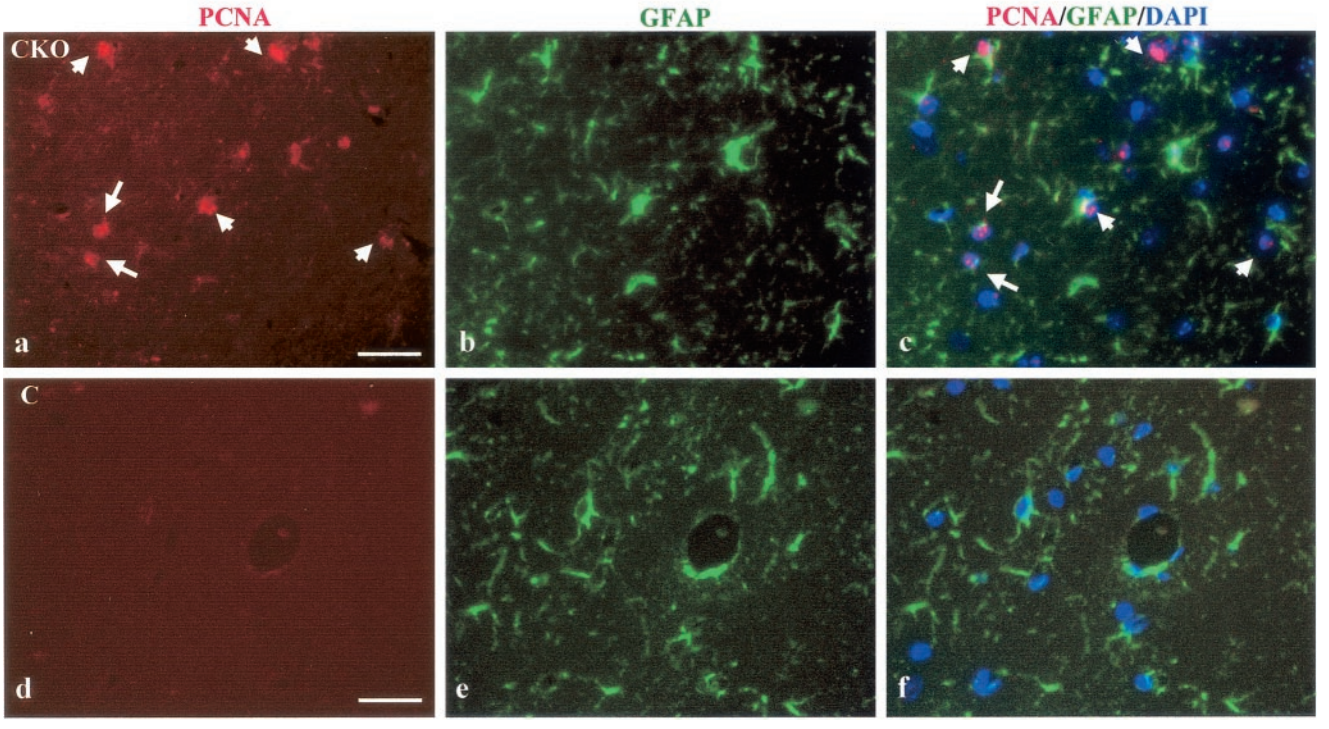

FIG. 6. Increased astrocyte number in the brains of *Nf1*^{GFAP}*CKO* mice is the result of increased astrocyte proliferation. PCNA immunofluorescence identifies proliferating cells (red) in the CA1 region of the hippocampus of adult *Nf1*^{GFAP}*CKO* (CKO) mice. White arrows point to representative PCNA-labeled cells (panel a). Almost no PCNA-immunoreactive proliferating cells were present in the hippocampus of control (C) mice (panel d). GFAP immunofluorescence (green) of astrocytes in the CA1 region of the hippocampus is shown for CKO mice (panel b) and for control mice (panel e). Note that there are increased numbers of astrocytes in panel b, corresponding to the mutant mice, compared to panel e (control mice). Merged PCNA/GFAP/DAPI images are shown for CKO (panel c) and control (panel f) mice. The nuclei of the cells in these images are stained with DAPI and appear dark blue. The white arrows in the merged PCNA/GFAP/DAPI (panel c) for the *Nf1*^{GFAP}*CKO* mice denote several double-labeled GFAP-positive astrocytes with PCNA-labeled nuclei (pink). No GFAP/PCNA/DAPI-immunolabeled cells are observed in the hippocampus of control mice (panel f).

als with NF1 develop astrocytomas at an increased frequency, and loss of neurofibromin is observed in symptomatic NF1-associated but not sporadic pilocytic astrocytomas (19, 25, 28, 30, 38). Collectively, these findings argue that *NF1* inactivation is associated with NF1 astrocytoma formation but do not address the fundamental issue of whether neurofibromin loss is necessary and sufficient for astrocytoma development. In an effort to determine the contribution of neurofibromin to NF1 astrocytoma formation, we analyzed the effect of *Nf1* inactivation in mouse astrocytes at various developmental times in vitro and in vivo. Our results suggest that *Nf1* loss provides a clear growth advantage for astrocytes in vitro and in vivo but is not sufficient for astrocytoma formation in mice.

Over the past few years, several transgenic lines of GFAP-Cre mice have been developed that demonstrate Cre expression in astrocytes, but there is also considerable ectopic expression in several populations of neurons and a few other cell types. By using the 2.2-kb fragment of either the mouse or human GFAP promoter for the generation of Cre transgenic mice, Cre expression was found primarily in astrocytes but also in subpopulations of neurons in the hippocampus, dentate gyrus, cortex, and cerebellum (33; K. Akassoglou and G. Kolias, 1999, Cre transgenic database [http://www.mshri.on.ca/nagy/Cre-being.htm]; A. Messing, 1997, Cre transgenic database). The GFAP-Cre mice developed by Messing and coworkers exhibit Cre expression in neural precursor cells as early as embryonic day 10.5 (Zhu et al., unpublished data). Similar results were also observed with other GFAP-Cre mice, in which predominantly neuronal rather than astrocyte-specific expression was detected (27).

In contrast, our GFAP-Cre transgenic lines demonstrated robust astrocyte expression by embryonic day 14.5 but did not have transgene expression in neurons, oligodendrocytes, or Schwann cells. Based on these results, it is likely that our *Nf1*^{GFAP}*CKO* mice represent a good model of astrocyte-specific *Nf1* inactivation in the central nervous system.

The lack of astrocyte tumor formation in these *Nf1*^{GFAP}*CKO* mice may reflect several possibilities. First, *Nf1* inactivation leads to tumor formation only if it occurs at the correct developmental time. To address this possibility, we analyzed the effect of *Nf1* loss at several developmental times, including embryonic days 12.5 and 14.5 as well as postnatal day 2. This was accomplished by preparing astrocyte cultures from conventional *Nf1*$^{-/-}$ mice at embryonic day 12.5 as well as postnatal day 2 *Nf1flox/flox* cultures with *Nf1* inactivation by Cre-adenovirus in vitro. In addition, *Nf1* inactivation occurred in vivo by E14.5 in the *Nf1*^{GFAP}*CKO* mice detailed in this report, at a time that coincides with type I astrocyte differentiation, and by E10.5 in the *Nf1*^{GFAP}*CKO* mice generated by Parada and associates (Zhu et al., unpublished data). Although these

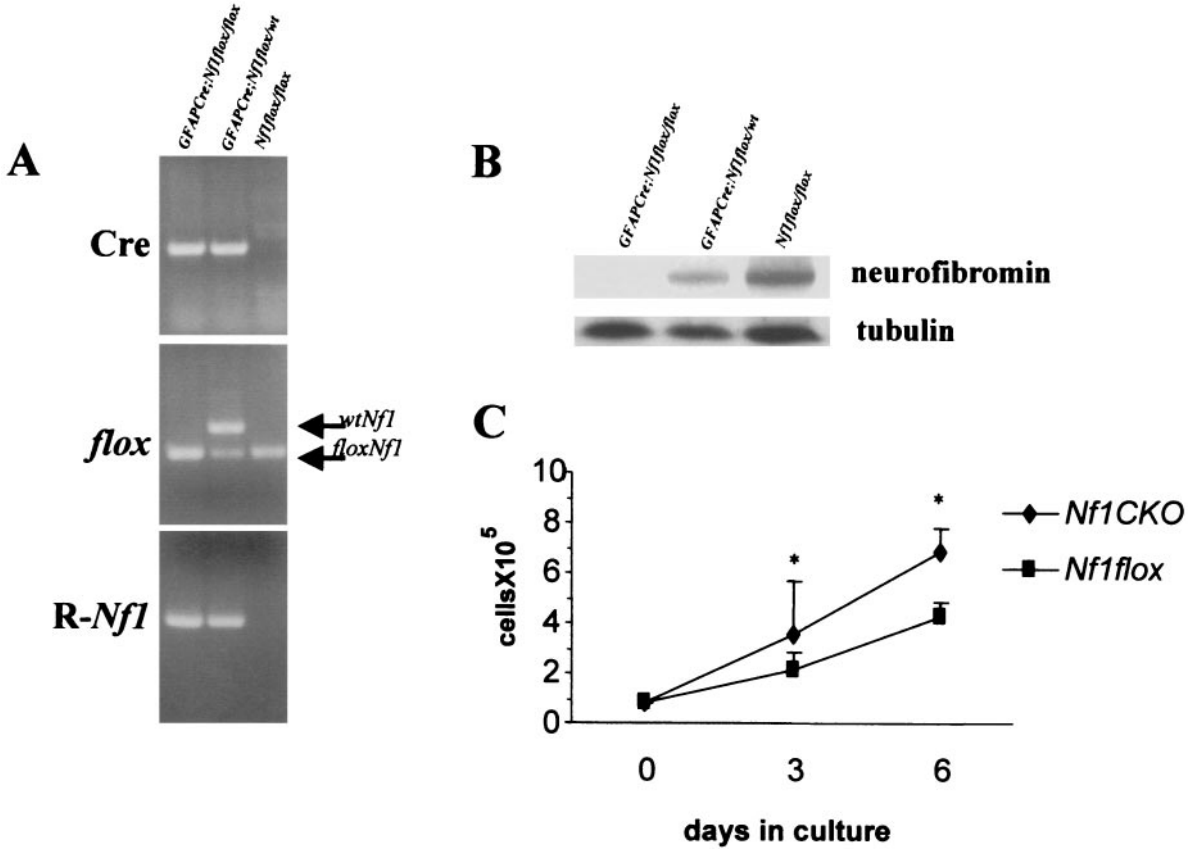

FIG. 7. Inactivation of *Nf1* influences the growth but not the tumorigenic properties of astrocytes derived from *Nf1*^{GFAP}*CKO* mice in vitro. (A) Cultured astrocytes were tested by PCR with specific primers to detect the presence of the Cre transgene, the conditional *Nf1flox* allele, and the recombined *Nf1* allele. The recombined *Nf1* allele (*R-Nf1*), as a result of Cre-mediated recombination of the conditional allele (*floxNf1*), is detected only in astrocytes that contain the Cre transgene (lanes 1 and 2) derived from astrocyte-specific *Nf1* knockout mice. (B) Neurofibromin protein expression is lost in astrocytes in culture derived from the brains of GFAP-Cre *Nf1flox/flox* (*Nf1*^{GFAP}*CKO*) mice and reduced in astrocytes derived from GFAP-Cre *Nf1flox/wt* mice compared with astrocytes from the *Nf1flox/flox* littermates. (C) Cultured astrocytes derived from *Nf1*^{GFAP}*CKO* mice (*Nf1CKO*) show a growth advantage in comparison with control *Nf1flox/flox* (*Nf1flox*) astrocytes.

three different *Nf1*-deficient astrocyte populations exhibited defects in their growth properties, they lacked tumorigenic properties and could not induce astrocytoma formation when implanted intracranially in the brains of immunocompromised mice.

During development, neurofibromin expression in rodent embryos is first detected uniformly in all tissues by day 10, including neuroglial precursor populations (22, 35). During embryonic development and in the adult, neurofibromin expression in the nervous system is highest in neurons with comparatively very low levels of expression in astrocytes. Studies are under way to investigate the relationship between neurofibromin expression and astroglial cell differentiation.

Second, p21^{ras} activation may not provide sufficient mitogenic signaling for astrocyte transformation. This possibility was evaluated in our previous studies, in which transgenic mice that express an oncogenic p21^{ras} (RAS^{G12V}) molecule specifically in astrocytes (B8 RAS transgenic mice) were generated. These B8 mice demonstrated massive astrocyte proliferation throughout the brain and developed high-grade astrocytomas around 3 to 4 months of age (13). Analysis of these tumors demonstrated a number of secondary "cooperating" genetic changes previously reported in human high-grade astrocytomas, including loss of p16, p53, and PTEN/MMAC1 as well as increased expression of CDK4 and the epidermal growth factor receptor. The reason that the B8 RAS transgenic mice develop high-grade astrocytomas while *Nf1*^{GFAP}*CKO* mice do not likely reflects the fact that we overexpressed a constitutively activated p21^{ras} molecule at high levels sufficient to initiate transformation, which may have resulted in secondary genetic changes. This high, nonphysiological level of p21^{ras} activation was not achieved in the *Nf1*^{GFAP}*CKO* mice.

Third, it is possible that additional genetic events in combination with *Nf1* inactivation might be required for NF1-associated astroglial tumorigenesis. Previous work by Jacks and colleagues has shown that combined *Nf1* and p53 loss can lead to the formation of high-grade malignant astrocytomas (39). Since individuals with NF1 develop low-grade astrocytomas, and not high-grade malignant gliomas, it is unlikely that p53 loss is the critical genetic event in NF1-associated astrocytoma formation. In this regard, p53 mutations are not typically detected in NF1-associated or sporadic pilocytic astrocytomas (23, 30). Recent studies from our laboratory with gene expression profiling of NF1-associated pilocytic astrocytomas have demonstrated significant alterations in the expression of genes involved in cell adhesion, motility, and actin cytoskeleton-as-

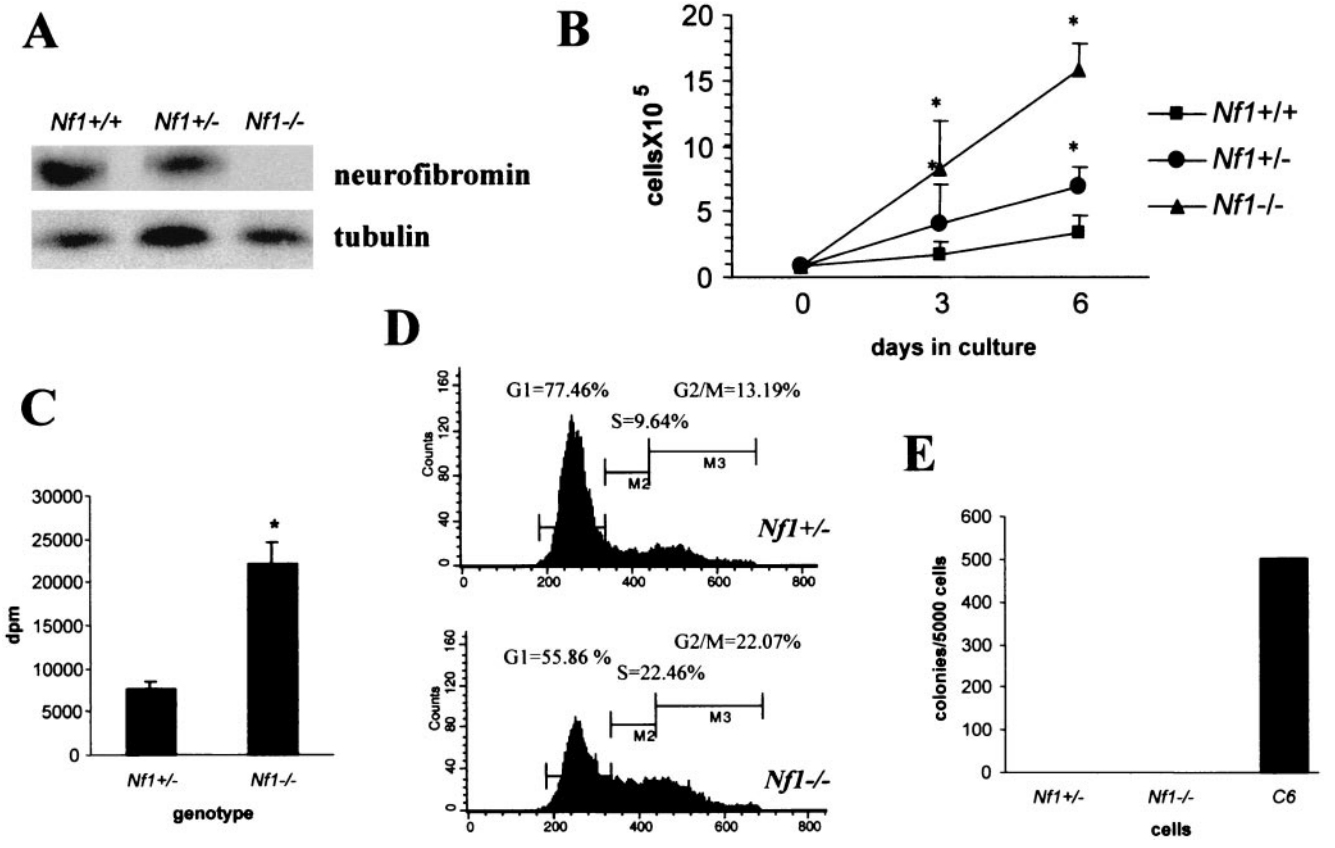

FIG. 8. Embryonic day 12.5 $Nf1^{-/-}$ astroglial cells show a significant increase in growth in vitro but lack tumorigenic properties. (A) Western blotting of astroglial cell extracts with an antineurofibromin antibody demonstrated loss of neurofibromin in $Nf1^{-/-}$ astroglial cells. (B) Growth curves of $Nf1^{-/-}$, $Nf1^{+/-}$, and $Nf1^{+/+}$ astrocytes showed a significant growth advantage for $Nf1^{-/-}$ astroglial cells at 3 and 6 days in culture. (C) When stimulated with fetal bovine serum, $Nf1^{-/-}$ astroglial cells showed increased [^{3}H]thymidine incorporation in comparison with $Nf1^{+/-}$ astrocytes. (D) The growth advantage observed by cell counting and [^{3}H]thymidine incorporation was also demonstrated by flow cytometry analysis of the cell cycle of $Nf1^{-/-}$ and $Nf1^{+/-}$ cells. (E) $Nf1^{-/-}$ and $Nf1^{+/-}$ astroglial cells do not form colonies in soft agar. C6 glioma cells were used as a positive control in the soft agar assay.

sociated processes (20). These changes are not seen in $Nf1^{-/-}$ astrocytes and may reflect some of the additional genetic changes associated with NF1 astrocytoma tumorigenesis. Further work will be necessary to determine whether these changes in combination with *NF1* inactivation are necessary and sufficient for NF1-associated astrocytoma formation or whether they merely represent gene expression changes associated with NF1 astrocytoma development.

Fourth, conventional models of astrocytomas employ the GFAP promoter, which drives expression of transgenes in GFAP-immunoreactive type 1 fibrillary astrocytes. It is conceivable that NF1-associated low-grade (pilocytic) astrocytomas do not arise from type 1 fibrillary astrocytes, but rather from a different cell of origin. Several studies have highlighted the inherent differences between pilocytic astrocytomas and high-grade fibrillary astrocytomas, with regard to both genetic changes and glial cell protein expression patterns (11, 30, 40, 44, 47). For instance, pilocytic astrocytomas express the unique PEN5 epitope shared with cells and tumors of an oligodendrocyte lineage (15). This marker is not expressed in fibrillary astrocytes or astrocytomas. Recent studies from our laboratory have demonstrated expression of oligodendrocyte-associated transcripts, such as PLP, PMP-22, MBP, and oligodendrocyte myelin glycoprotein in pilocytic astrocytomas, suggesting that these NF1-associated tumors exhibit some gene expression features of oligodendrocyte type 2 astrocyte cells (20). In this regard, it may be necessary to inactivate *Nf1* in the correct progenitor cell, perhaps an oligodendrocyte type 2 astrocyte or glial restricted precursor cell, in order to generate NF1-associated astrocytomas in mice.

Fifth, it is possible that NF1-associated astrocytoma formation requires a permissive brain environment. In children with NF1, grade I astrocytomas are most frequently found in the optic pathway (31). It is possible that *Nf1* inactivation in specific populations of astrocytes in the brain is required. In this regard, astrocytes from different regions of the brain may have different functional properties. Astrocytes from different regions of the brain have been reported to have different responses to agents that elevate cyclic AMP, regional specificity in gap junction coupling (29), differences in glutamate and serotonin uptake (1), and distinctive growth patterns (14). A more detailed analysis of the eyes and optic nerves of $Nf1^{GFAP}CKO$ mice is presently under way.

Similarly, NF1-associated astrocytomas form in the brains of children in which the surrounding cellular milieu is heterozygous for a germ line *NF1* mutation. It is possible that NF1

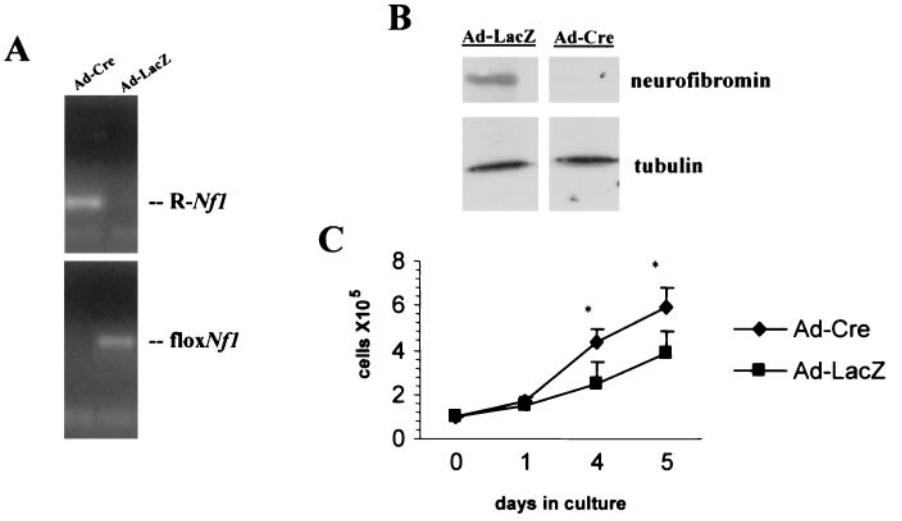

FIG. 9. Postnatal day 2 $Nf1^{-/-}$ astroglial cells show a significant increase in growth in vitro but lack tumorigenic properties. (A) Cre-adenovirus (Ad-Cre) treatment of astrocytes in culture results in Cre-mediated recombination of the *Nf1flox* allele (*floxNf1*) and formation of the recombined allele (*R-Nf1*), whereas no recombination is observed in astrocytes infected with a control LacZ adenovirus (Ad-LacZ). (B) No expression of the *Nf1* protein (neurofibromin) was detected in *Nf1flox/flox* astrocytes after Ad5-Cre infection. The protein levels are not affected when *Nf1flox/flox* astrocytes are infected with Ad5-LacZ virus. (C) Ad5-Cre-infected *Nf1flox/flox* astrocytes (Ad-Cre) show a growth advantage compared with Ad5-LacZ-infected *Nf1flox/flox* astrocytes (Ad-LacZ).

astrocytoma formation requires that the brain environment contain $Nf1^{+/-}$ cells. To address the possibility that astrocytoma formation in $Nf1^{GFAP}CKO$ mice might require an $Nf1^{+/-}$ brain environment, we are in the process of generating GFAP-Cre $Nf1^{flox/mut}$ mice, in which the brain is $Nf1^{+/-}$ but the astrocytes are $Nf1^{-/-}$. In addition, experiments are under way to examine the effect of intracranial implantation of $Nf1^{-/-}$ astrocytes into the brains of $Nf1^{+/-}$ mice on astrocytoma formation. To date, $Nf1^{+/-}$ mice in which *Nf1*-deficient astrocytes have been intracranially implanted are healthy and asymptomatic after 6 months (L. Fink, Y. L. Wu, and D. H. Gutmann, unpublished observations).

In summary, our studies emphasize that neurofibromin is an important growth regulator for astrocytes but that astrocytoma formation may require more complex interactions involving cooperating genetic events and a permissive brain environment. Further work on the relationship between neurofibromin function, astrocyte growth regulation, and pilocytic astrocytoma formation should yield critical insights into the molecular pathogenesis of NF1-associated astrocytomas and result in the development of essential preclinical mouse models for specific features of the human disease.

ACKNOWLEDGMENTS

This work was supported by funding from the National Institutes of Health (NS36996 to D.H.G.). M.L.B. is supported by a National Research Service Award fellowship from the National Eye Institute (1F32 EY14039-01).

We thank S. K. Song for the MRI studies as well as YanLi Wu, Lisa Fink, Sean Brophy, and Rebecca Baldwin for technical assistance during the execution of these experiments. We thank Abhijit Guha, David Holtzman, Alexander Parsadanian, Selva Baltan-Tekkok, Mercedes Salvador, and Rosario Hernandez for comments and discussions. We also thank Anthony Apicelli for helpful discussions.

REFERENCES

1. **Amundson, R. H., S. K. Goderlie, and H. K. Kimelberg.** 1992. Uptake of ^{3}H-serotonin and ^{3}H-glutamate by primary astrocyte cultures. II. Differences in cultures prepared from different brain regions. Glia **6:**9–18.
2. **Anton, M., and F. L. Graham.** 1995. Site-specific recombination mediated by an adenovirus vector expressing the cre recombinase protein: a molecular switch for control of gene expression. J. Virol. **69:**4600–4606.
3. **Bajenaru, M. L., J. Donahoe, T. Corral, K. M. Reilly, S. Brophy, A. Pellicer, and D. H. Gutmann.** 2001. Neurofibromatosis 1 (NF1) heterozygosity results in a cell-autonomous growth advantage for astrocytes. Glia **33:**314–323.
4. **Ballester, R., D. A. Marchuk, M. Boguski, A. M. Saulino, R. Letcher, M. Wigler, and F. S. Collins.** 1990. The NF1 locus encodes a protein functionally related to mammalian GAP and yeast IRA proteins. Cell **63:**851–859.
5. **Basu, T. N., D. H. Gutmann, J. A. Fletcher, T. W. Glover, F. S. Collins, and J. Downward.** 1992. Aberrant regulation of ras proteins in tumour cells from type 1 neurofibromatosis patients. Nature **356:**713–715.
6. **Bollag, G., and F. McCormick.** 1991. Regulators and effectors of ras proteins. Annu. Rev. Cell Biol. **7:**601–632.
7. **Bollag, G., D. W. Clapp, S. Shih, F. Adler, Y. Y. Zhang, P. Thompson, B. J. Lange, M. H. Freedman, F. McCormick, T. Jacks, and K. Shannon.** 1996. Loss of NF1 results in activation of the Ras signaling pathway and leads to aberrant growth in haematopoietic cells. Nat. Genet. **12:**144–148.
8. **Brannan, C. I., A. S. Perkins, K. S. Vogel, N. Ratner, M. L. Nordlund, S. W. Reid, A. M. Buchberg, N. A. Jenkins, L. F. Parada, and N. G. Copeland.** 1994. Targeted disruption of the neurofibromatosis type-1 gene leads to developmental abnormalities in heart and various neural crest-derived tissues. Genes Dev. **8:**1019–1029.
9. **Brenner, M., and A. Messing.** 1996. GFAP transgenic mice. Methods **10:** 351–364.
10. **Cawthon, R. M., M. Weiss, G. Xu, D. Viskochil, M. Culver, J. Stevens, M. Robertson, D. Dunn, R. Gesteland, P. O'Connell, and R. White.** 1990. A major segment of the neurofibromatosis 1 gene: cDNA sequence, genomic structure and point mutations. Cell **62:**193–201.
11. **Cheng, Y., J. C. S. Pang, H.-K. Ng, M. Ding, S. F. Zhang, J. Zheng, D. G. Liu, and W. S. Poon.** 2000. Pilocytic astrocytomas do not show most of the genetic changes commonly seen in diffuse astrocytomas. Histopathology **37:**437–444.
12. **DeClue, J. E., A. G. Papageorge, J. A. Fletcher, S. R. Diehl, N. Ratner, W. C. Vass, and D. R. Lowy.** 1992. Abnormal regulation of mammalian p21^{ras} contributes to malignant tumor growth in von Recklinghausen (type 1) neurofibromatosis. Cell **69:**265–273.
13. **Ding, H., L. Roncari, P. Shannon, S. MacMaster, X. Wu, N. Lau, J. Karaskova, D. H. Gutmann, J. A. Squire, A. Nagy, and A. Guha.** 2001. Astrocyte-specific expression of activated Ras results in malignant astrocytomas in a transgenic mouse model of human gliomas. Cancer Res. **61:**3826–3836.
14. **Escalona-Zapara, J., and M. D. Diez-Nau.** 1981. Distinctive growth patterns

between cerebral and cerebellar astrocytomas—a tissue culture study. Histopathology **5:**639–650.
15. **Figarella-Branger, D., L. Daniel, P. Andre, S. Guia, W. Renaud, G. Monti, E. Vivier, and G. Rougon.** 1999. The PEN5 epitope identifies an oligodendrocyte precursor cell population and pilocytic astrocytomas. Am. J. Pathol. **155:**1261–1269.
16. **Friedman, J. M., D. H. Gutmann, M. M. MacCollin, and V. M. Riccardi (ed.).** 1999. Neurofibromatosis, 3rd ed. Johns Hopkins Press, Baltimore, Md.
17. **Gutmann, D. H., D. L. Wood, and F. S. Collins.** 1991. Identification of the neurofibromatosis type 1 gene product. Proc. Natl. Acad. Sci. USA **21:**9658–9662.
18. **Gutmann, D. H., A. Loehr, Y. Zhang, J. Kim, M. Henkemeyer, and A. Cashen.** 1999. Haploinsufficiency for the neurofibromatosis 1 (NF1) tumor suppressor results in increased astrocyte proliferation. Oncogene **18:**4450–4459.
19. **Gutmann, D. H., J. Donahoe, T. Brown, C. D. James, and A. Perry.** 2000. Loss of neurofibromatosis 1 (NF1) gene expression in NF1-associated pilocytic astrocytomas. Neuropathol. Exp. Neurobiol. **26:**361–367.
20. **Gutmann, D. H., N. M. Hedrick, J. Li, R. Nagarajan, A. Perry, and M. A. Watson.** 2002. Comparative gene expression profile analysis of neurofibromatosis 1 (NF1)-associated and sporadic pilocytic astrocytomas. Cancer Res. **62:**2085–2091.
21. **Hewett, S. J., D. W. Choi, and D. H. Gutmann.** 1995. Increased expression of the neurofibromatosis 1 (NF1) tumor suppressor gene protein, neurofibromin, in reactive astrocytes in vitro. Neuroreport **6:**1505–1508.
22. **Huynh, D. P., T. Nechiporuk, and S. M. Pulst.** 1994. Differential expression and tissue distribution of type I and type II neurofibromins during mouse fetal development. Dev. Biol. **161:**538–551.
23. **Ishii, N., Y. Sawamura, M. Tada, D. M. Daub, R. C. Janzer, M. Meagher-Villemure, N. de Tribolet, and E. G. Van Meir.** 1998. Absence of p53 gene mutations in a tumor panel representative of pilocytic astrocytoma diversity by using a p53 functional assay. Int. J. Cancer **76:**797–800.
24. **Jacks, T., T. S. Shih, E. M. Schmitt, R. T. Bronson, A. Bernards, and R. A. Weinberg.** 1994. Tumor predisposition in mice heterozygous for a targeted mutation in NF1. Nat. Genet. **7:**353–361.
25. **Kluwe, L., C. Hagel, M. Tatagiba, S. Thomas, D. Stavrou, H. Ostertag, A. von Deimling, and V. F. Mautner.** 2001. Loss of NF1 alleles distinguish sporadic from NF1-associated pilocytic astrocytomas. J. Neuropathol. Exp. Neurol. **60:**917–920.
26. **Kolb, A. F., and S. G. Siddell.** 1996. Genomic targeting with an MBP-Cre fusion protein. Gene **183:**53–60.
27. **Kwon, C. H., X. Zhu, J. Zhang, L. L. Knoop, R. Tharp, R. J. Smeyne, C. G. Eberhart, P. C. Burger, and S. J. Baker.** 2001. Pten regulates neuronal soma size: a mouse model of Lhermitte-Duclos disease. Nat. Genet. **29:**404–411.
28. **Lau, N., M. M. Feldkamp, L. Roncari, A. H. Loehr, P. Shannon, D. H. Gutmann, and A. Guha.** 2000. Loss of neurofibromin is associated with activation of the RAS/MAPK and PI3-K/AKT signaling in neurofibromatosis 1 astrocytoma. J. Neuropathol. Exp. Neurol. **59:**759–767.
29. **Lee, S. H., W. T. Kim, A. H. Cornell-Bell, and H. Sontheimer.** 1994. Astrocytes exhibit regional specificity in gap-junction coupling. Glia **11:**315–325.
30. **Li, J., A. Perry, C. D. James, and D. H. Gutmann.** 2001. Cancer related gene expression in neurofibromatosis 1 (NF1)-associated pilocytic astrocytomas. Neurology **56:**885–890.
31. **Listernick, R., D. N. Louis, R. J. Packer, and D. H. Gutmann.** 1997. Optic pathway gliomas in children with neurofibromatosis 1: consensus statement from the NF1 optic pathway glioma task force. Ann. Neurol. **41:**143–149.
32. **Lobe, C. G., K. E. Koop, W. Kreppner, H. Lomeli, M. Gertsenstein, and A. Nagy.** 1999. Z/AP, a double reporter for cre-mediated recombination. Dev. Biol. **208:**281–292.
33. **Marino, S., M. Vooijs, H. van der Gulden, J. Jonkers, and A. Berns.** 2000. Induction of medulloblastomas in p53-null mice by somatic inactivation of Rb in the external granular layer cells of the cerebellum. Genes Dev. **14:**994–1004.
34. **Martin, G. A., D. Viskochil, G. Bollag, P. C. McCabe, W. J. Crosier, H. Haubruck, L. Conroy, R. Clark, P. O'Connell, R. M. Cawthon, M. A. Innis, and F. McCormick.** 1990. The GAP-related domain of the neurofibromatosis type 1 gene product interacts with ras p21. Cell **63:**843–849.
35. **Nordlund, M. L., T. A. Rizvi, C. I. Brannan, and N. Ratner.** 1995. Neurofibromin expression and astrogliosis in neurofibromatosis (type 1) brains. J. Neuropathol. Exp. Neurol. **54:**588–600.
36. **Norton, K. K., R. T. Geist, D. K. Mahadeo, and D. H. Gutmann.** 1996. Expression of the neurofibromatosis 1 (NF1) tumor suppressor gene product, neurofibromin, during growth arrest in fibroblasts. Neuroreport **7:**601–604.
37. **Paxinos, G., and C. Watson.** 1986. The rat brain in stereotaxic coordinates, 2nd ed. Academic Press, New York, N.Y.
38. **Platten, M., M. J. Giordano, C. M. F. Dirvem, D. H. Gutmann, and D. N. Louis.** 1996. Upregulation of specific NF1 gene transcripts in sporadic pilocytic astrocytomas. Am. J. Pathol. **149:**621–627.
39. **Reilly, K. M., D. A. Loisel, R. T. Bronson, M. E. McLaughlin, and T. Jacks.** 2000. Nf1;Trp53 mutant mice develop glioblastoma with evidence of strain-specific effects. Nat. Genet. **26:**109–113.
40. **Sanoudou, D., O. Tingby, M. A. Ferguson-Smith, V. P. Collins, and N. Coleman.** 2000. Analysis of pilocytic astrocytomas by comparative genomic hybridization. Br. J. Cancer **82:**1218–1222.
41. **Stec, D. E., R. L. Davisson, R. E. Haskell, B. L. Davidson, and C. D. Sigmund.** 1999. Efficient liver-specific deletion of a floxed human angiotensin transgene by adenoviral delivery of Cre recombinase in vivo. J. Biol. Chem. **274:**21285–21290.
42. **Viskochil, D., A. M. Buchberg, G. Xu, R. M. Cawthon, J. Stevens, R. K. Wolff, M. Culver, J. C. Carey, N. G. Copeland, N. A. Jenkins, and R. White.** 1990. Deletions and translocation interrupt a cloned gene at the neurofibromatosis 1 locus. Cell **62:**187–192.
43. **Wallace, M. R., D. A. Marchuk, L. B. Andersen, R. Letcher, H. M. Odeh, A. M. Saulino, J. W. Fountain, A. Brereton, J. Nicholson, A. L. Mitchell, and F. S. Collins.** 1990. Type 1 neurofibromatosis gene: identification of a large transcript disrupted in NF1 patients. Science **249:**181–186.
44. **White, F. V., D. C. Anthony, E. J. Yunis, N. J. Tarbell, R. M. Scott, and D. E. Schofield.** 1995. Nonrandom chromosomal gains in pilocytic astrocytomas of childhood. Hum. Pathol. **26:**979–986.
45. **Xu, G., B. Lin, K. Tanaka, D. Dunn, D. Wood, R. Gesteland, R. White, R. Weiss, and F. Tamanoi.** 1990. The catalytic domain of the neurofibromatosis type 1 gene product stimulates ras GTPase and complements ira mutants of S. cerevisiae. Cell **63:**835–841.
46. **Zaidi, A. U., H. Enomoto, J. Milbrandt, and K. A. Roth.** 2000. Dual fluorescent in situ hybridization and immunohistochemical detection with tyramide signal amplification. J. Histochem. Cytochem. **48:**1369–1375.
47. **Zattara-Cannoni, H., D. Gambarelli, G. Lena, H. Dufour, M. Choux, F. Grisoli, and A. M. Vagner-Capodano.** 1998. Are juvenile pilocytic astrocytomas benign tumors? A cytogenetic study in 24 cases. Cancer Genet. Cytogenet. **104:**157–160.
48. **Zhu, Y., M. I. Romero, P. Ghosh, Z. Ye, P. Charnay, E. J. Rushing, J. D. Marth, and L. Parada.** 2001. Ablation of NF1 function in neurons induces abnormal development of the cerebral cortex and reactive gliosis in the brain. Genes Dev. **15:**859–876.